RSC Advances

ROYAL SOCIETY OF CHEMISTRY

www.rsc.org/advances

Journal Name

ARTICLE

Significantly improved de/rehydrogenation properties of lithium borohydride modified with hexagonal boron nitride†

Received 00th January 20xx,
Accepted 00th January 20xx

DOI: 10.1039/x0xx00000x

www.rsc.org/

Guoping Tu, Xuezhang Xiao, Teng Qin, Yiqun Jiang, Shouquan Li, Hongwei Ge and Lixin Chen*

The remarkable hydrogen de/absorption properties of lithium borohydride are achieved by mechanical milling $LiBH_4$ with hexagonal boron nitride (h-BN). It is found that the dehydrogenation properties of $LiBH_4$ are improved with increasing the amount of h-BN. The 30 mol% h-BN doped $LiBH_4$ composite starts to release hydrogen form just 180 °C, which is 100 °C lower than the onset dehydrogenation temperature of ball milled $LiBH_4$. Moreover, the 30 mol% h-BN doped $LiBH_4$ composite can release 12.6 wt% hydrogen in 2h at 400 °C, while only 0.98 wt% H_2 is gained from ball milled $LiBH_4$. The apparent activation energy (E_a) of hydrogen desorption had been reduced from 198.31 kJ/mol for ball milled $LiBH_4$ to 155.8 kJ/mol for 30 mol% h-BN doped $LiBH_4$. In addition, the rehydrogenation of the composite is achieved under 400 °C and 10 MPa of H_2. These remarkable results are largely attributed to the lone pair electrons of nitrogen induced destabilization of $LiBH_4$ and their heterogeneous nucleation.

1. Introduction

Lithium borohydride ($LiBH_4$) have been widely investigated as a candidate for hydrogen storage materials due to its large hydrogen capacity (13.8 wt%) and volumetric hydrogen density (121 kg/m^3)[1-3]. The decomposition of $LiBH_4$ undergoes multiple stages[4], including polymorphic transformation at about 110 °C, melting at about 280 °C with a slight accompanying hydrogen desorption, and then the main evolution of hydrogen at 400-600 °C [5, 6]. This major decomposition reaction is [7] :

$LiBH_4 \rightarrow LiH + B + 3/2H_2$ (1)

Consequently, the desorption temperature of pristine $LiBH_4$ is higher than the desired value. Therefore, it is worthwhile to study strategies to reduce the thermodynamic stability and the hydrogen desorption kinetics of $LiBH_4$.

Since Züttel et al.[1] reported that $LiBH_4$ doped with SiO_2 desorbs hydrogen below 200 °C, a lower temperature than for bulk $LiBH_4$. Various potential dopants/catalysts, including metals, metal halides, and metal oxides, have been tentatively added into $LiBH_4$ to enhance its hydrogen storage properties. The metal, such as Mg[8], Al[9], Ni[10], Ti, V, Cr and Sc[11], did not greatly improve the dehydrogenation properties of $LiBH_4$, indicating a temperature requirement higher than 400 °C for fast hydrogen desorption and slow dehydrogenation kinetics. Taking Al doped with $LiBH_4$ for example, 7.2 wt% hydrogen was released at 450 °C, and completing the dehydrogenation would take above 30 hours[9, 11, 12]. For the metal halides doped $LiBH_4$, the dehydrogenation temperature was considerably decreased to 220-300 °C by doped with $FeCl_2$, $CoCl_2$, $NiCl_2$ [13], $LaCl_3$, $CeCl_3$, LaF_3 and CeF_3 [14], and even to about 100 °C by mixing with TiF_3 [15], $TiCl_3$ [16] and ZnF_2 [17]. However by-product including harmful diborane also will release, and thus results in drastically degraded reversible hydrogen capacity[18]. By doping with metal oxides, such as Fe_2O_3, V_2O_5, Nb_2O_5, TiO_2[19], $LiBH_4$ was able to dehydrogenate at much lower temperatures[20-22]. For example, 6 wt% hydrogen could be released at 200 °C for a $LiBH_4$-Fe_2O_3 mixture with a mass ratio of 1:2[20]. Unfortunately the destabilization of $LiBH_4$ by metal oxides resulted from a redox reaction, which caused $LiBH_4$ could not be rehydrogenated under moderate conditions[20].

In this paper, the hydrogen storage properties of $LiBH_4$ defined by doping with h-BN were investigated. We observed that the dehydrogenation properties of $LiBH_4$ are improved by doping with h-BN. It is found that h-BN addition greatly facilitates the dehydrogenation kinetics of $LiBH_4$, and the rehydrogenation properties are also enhanced. This improvement may be correlated to the lone pair electrons of nitrogen induced destabilization of $LiBH_4$ and a heterogeneous nucleation process of the solid decomposition products of reaction (1) on the surface of BN.

2. Experimental Section

Commercial hexagonal boron nitride (99%, Aladdin), and $LiBH_4$ (95%, Acros Organics) were used in this research without further purification. Samples of $LiBH_4$ and x h-BN (x=0, 0.05, 0.15, 0.3, 0.5) were ball milled under a hydrogen pressure of 3

* State Key Laboratory of Silicon Materials, Key Laboratory of Advanced Materials and Applications for Batteries of Zhejiang Province, School of Materials Science and Engineering, Zhejiang University, Hangzhou 310027, China.
E-mail address: lxchen@zju.edu.cn (L.X. Chen). Tel./fax: +86 571 8795 1152.

† Electronic Supplementary Information (ESI) available: DSC curves with different rates and Isothermal dehydrogenation curves of the $LiBH_4$ doped with graphite. See DOI: 10.1039/x0xx00000x

MPa for 3h, The ball milling process was paused for 6 min every 24 min to avoid an increasing temperature of the samples. The as-synthesized samples were dehydrogenated at 400 °C under 0.1 MPa H_2 and rehydrogenated at 400 °C under 10 MPa of H_2. All experimental operations were performed in a high-pure Ar-filled glovebox.

The X-ray diffraction (XRD) analysis of the samples were performed on an X'Pert Pro (PANalytical, Netherlands) with Cu Kα radiation at 40 kV and 40 mA with the step size of 0.02° from 10° to 90° (2ϑ). Scanning electron microscopy (SEM, Hitachi SU-70) was performed to examine surface morphology of the samples. The microstructure was further examined by transmission electron microscopy (TEM, JEOL JEM-1200EX working at 200 kV) and high resolution transmission electron microscopy (HRTEM, FEI Tecnai G2 F20 S-Twin working at 200 kV). The differential scanning calorimetry and mass spectrometer (DSC-MS) measurements were conducted on a synchronous thermal analysis (Netzsch STA 449F3 analyzer/Netzsch Q403C mass spectrometer) with a heating rate of 5 K/min from room temperature to 500 °C under high purity argon condition with a purge rate of 50 ml/min. During the experiments the MS signals at m/z=2, 17, and 27 were recorded to detect possible evolving gases H_2, NH_3 and B_2H_6. Hydrogen desorption and absorption properties of the samples were quantitatively examined with volumetric method by a carefully calibrated Sievert's type apparatus. In order to compare with the hydrogen capacity of bulk $LiBH_4$, the hydrogen contents presented in this work are calculated based only on the $LiBH_4$.

3. Results and discussion

Fig. 1(a) shows the XRD patterns of pristine and ball milled h-BN. For both the pristine h-BN and ball milled h-BN, all the detected peaks can be assigned to the diffraction of h-BN phase according to JCPDS 34-0421. The sharp and intensity of diffraction peaks in Fig. 1(a) indicate the good crystallinity of h-BN as-received sample. However, after ball milling at 400 rpm for 3h, the diffraction peaks changed slightly, exhibited a little lower intensity and wider diffraction peaks. These may be ascribed to some amorphousization of h-BN happened, such as BN layers drifted during ball milling. The graphite-like structure of h-BN was studied by TEM and HRTEM, shown in Fig. 1(b) and Fig. 1(c). The TEM micrograph shows that the h-BN sample has a clear and flat surface. In the HRTEM image, the measured lattice fringes of ≈0.326 nm coincides with the lattice spacing of the (002) planes of the h-BN. The corresponding fast Fourier transform (FFT) analysis reveals hexagonal spots, indicating the structure of h-BN is hexagonal sheets[23].

Fig. 2 illustrates isothermal dehydrogenation curves of ball milled $LiBH_4$ and $LiBH_4$ doped with various amount of h-BN samples. The dehydrogenaton properties of $LiBH_4$ were markedly improved upon ball milling with h-BN, even addition

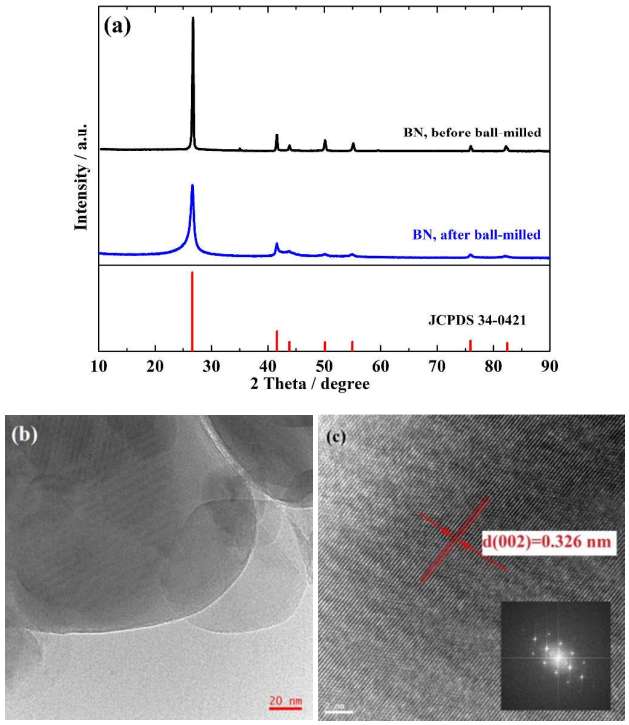

Fig. 1 (a) XRD patter of h-BN, (b) TEM image of h-BN and (c) HRTEM images of h-BN.

amount of h-BN is only 5 mol% of $LiBH_4$, the dehydrogenation behavior is quite different form pure $LiBH_4$. Obviously, It could be found that the improvement effect on dehydrogenation properties of $LiBH_4$ increases with addition amount of h-BN. When the h-BN doping amounts add up to 30 mol% of $LiBH_4$, 12.6 wt% hydrogen can be released within 2 h at 400 °C, while only 0.98 wt% hydrogen can be gained for ball milled $LiBH_4$. More importantly, ball milled $LiBH_4$ finishes the decomposition will take about 6000 min, and it can be shorted to 180 min after doping with 30 mol% h-BN. Therefore, it can be concluded that the doped h-BN greatly enhanced the dehydrogenation kinetics of $LiBH_4$.

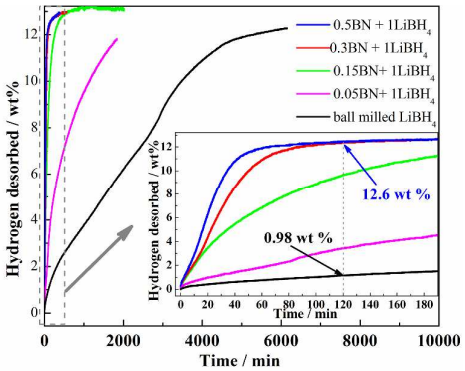

Fig. 2 (a) Isothermal dehydrogenation curves of ball milled $LiBH_4$ and $LiBH_4$ doped with different amount of h-BN at 400 °C

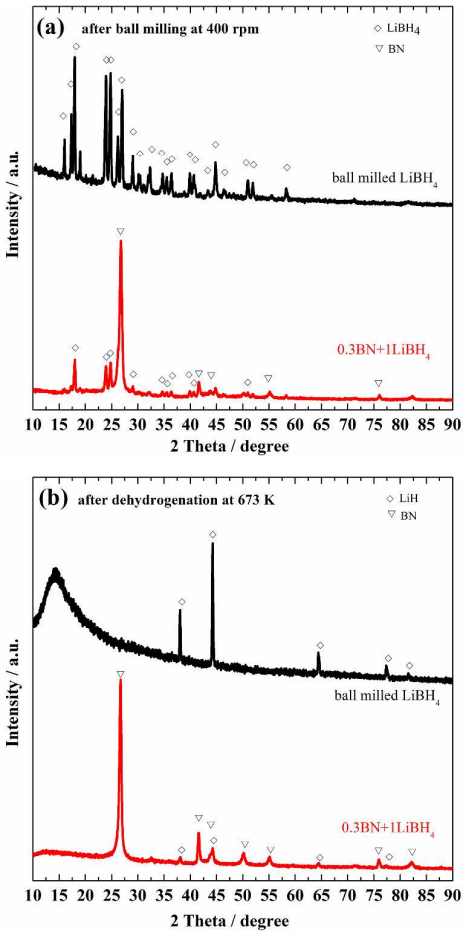

Fig. 3 XRD patterns of ball milled $LiBH_4$ and 30 mol% h-BN doped $LiBH_4$ samples: (a) after ball milling, (b) after dehydrogenation at 400 °C.

It is common knowledge that h-BN has very good chemical inertness, especially its resistance to acids and molten metals and its stability in air up to 1000 °C[23, 24]. And h-BN does not react with $LiBH_4$ neither after ball milling at 400 rpm nor after dehydrogenation at 400 °C. It is confirmed by the XRD patterns of $LiBH_4$ doped with h-BN samples, as shown in Fig. 3. The diffraction peaks of the samples after ball milling are corresponding to starting materials ($LiBH_4$ and h-BN), and after dehydrogenation the diffraction peaks are assigned to h-BN and LiH. LiH is the product of $LiBH_4$ decomposition.

The dehydrogenation property of the ball milled $LiBH_4$ and 30 mol% h-BN doped $LiBH_4$ samples were investigated by DSC-MS as shown in Fig. 4. As displayed in the DSC profiles, both ball milled $LiBH_4$ and 30 mol% h-BN doped $LiBH_4$ samples exhibit of four endothermic peaks during the heating process to 500 °C at 5 °C/min. The first endothermic peak around 113 °C corresponds to the phase transition of $LiBH_4$, and the second one around 285 °C is from melting of $LiBH_4$. The other two peaks at higher temperatures (350-500 °C) are attributed to the decomposition of $LiBH_4$ with hydrogen releases[1]. Obviously, after doping with h-BN, the melting of $LiBH_4$ shifted to the

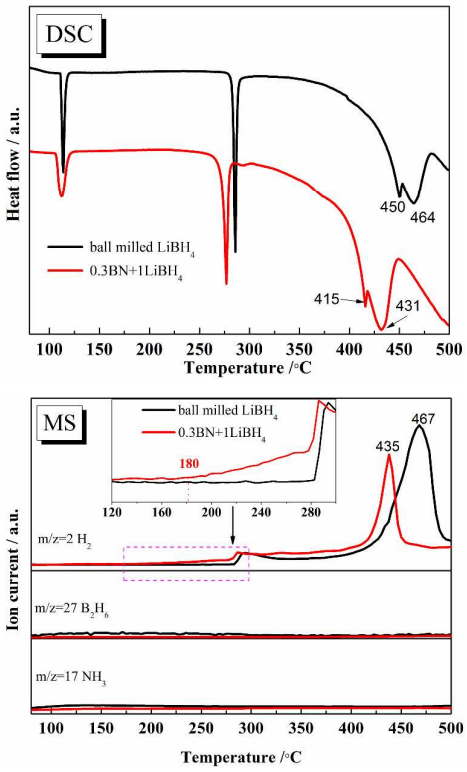

Fig. 4 DSC-MS profiles of ball milled $LiBH_4$ and 30 mol% doped h-BN $LiBH_4$ samples at a heating rate of 5 K/min.

lower temperature (276 °C), which may be due to $LiBH_4$ particle size reduces after ball milling with low density h-BN. The major dehydrogenation temperature of $LiBH_4$ reduces to 431 °C, lower than ball milled $LiBH_4$. From the MS profiles, only hydrogen was detected from the thermal desorption measurement by MS (data of possible B_2H_6, and NH_3 are shown in Fig. 4). The main hydrogen release peak are 467 °C and 435 °C for ball milled $LiBH_4$ and $LiBH_4$ doped with h-BN samples respectively, which is corresponding to the DSC results. With a careful analysis, we found that $LiBH_4$ begin releasing hydrogen at 180 °C, which is 100 °C lower than the onset dehydrogenation temperature of ball milled $LiBH_4$. We attribute the lower onset desorption temperature of $LiBH_4$ to the lone pair electrons of nitrogen atom on the h-BN surface, which may induce destabilization of $LiBH_4$ by the lone pair electrons complex with "electron-deficient" molecule $LiBH_4$ [25].

In order to gather better insight of the improvement on dehydrogenation kinetics of 30 mol% h-BN doped $LiBH_4$, apparent activation energy (E_a) related to the dehydrogenation of $LiBH_4$ was quantitatively determined by using the Kissinger's method according to Reaction (2)[26]:

$$\ln\left(\beta/T_p^2\right) = -E_a/RT_p + \ln(AR/E_a) \quad (2)$$

Where β (K/min) is the heating rate, T_p (K) is the absolute temperature at the maximum decomposition rate, E_a is the activation energy, A is the pre-exponential factor and R (8.314 $J \cdot mol^{-1} \cdot K^{-1}$) is the gas constant. In this work, T_p (K) are collected from the DSC curves with different rates for 5, 7.5, 10, 12.5, 15

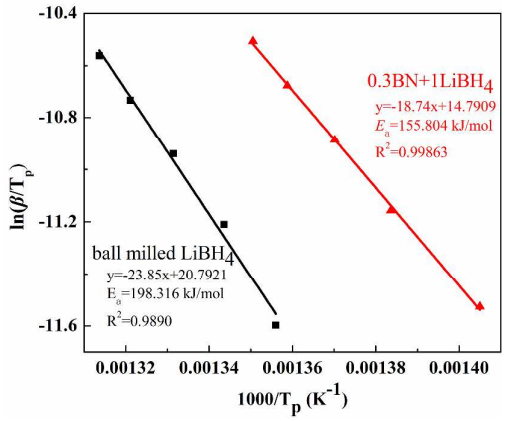

Fig. 5 Kissinger's plots obtained from the DSC data for the dehydrogenation of ball milled $LiBH_4$ and 30 mol% h-BN doped $LiBH_4$ samples

K/min, as shown in electronic supplementary information (ESI) Fig.S1†. Thus, the activation energy, E_a, can be obtained from the slope in a plot of $\ln(\beta/T_p^2)$ vs. $1000/T_p$. The apparent activation energy for the ball milled $LiBH_4$ dehydrogenation is estimated to 198.31 kJ/mol, which is in agreement with the previous report[27, 28]. The apparent activation energy of 30 mol% h-BN doped $LiBH_4$ dehydrogenation is estimated to be 155.80 kJ/mol, significantly lower than 198.31 kJ/mol of ball milled $LiBH_4$. These results provide quantitative evidence for h-BN additive can effectively improve the hydrogen desorption kinetics of $LiBH_4$.

The products of ball milled $LiBH_4$ and 30 mol% h-BN doped $LiBH_4$ samples after dehydrogenation were subsequently rehydrogenated at 400 °C under 10 MPa H_2 for 12 h. And the XRD patterns of rehydrogenation samples are presented in Fig. 6(a). The diffraction peaks of $LiBH_4$ doped with 30 mol% h-BN rehydrogenated samples are assigned to $LiBH_4$, h-BN and LiH, indicating that $LiBH_4$ was regenerated upon hydrogenation, even though the reverse reaction proceeded incompletely, due to the sequaration of a part of LiH and boron in the material after dehydrogenation[27]. However, without doping with h-BN, the diffraction peaks of $LiBH_4$ cannot be found in the rehydrogenation sample under the same condition, but some unknown and LiH diffraction peaks could be detected. The rehydrogenation of $LiBH_4$ has been reported only under harsh conditions such as 600 °C and 35 MPa H_2 [29, 30]. Meanwhile the rehydrogenation capacity of h-BN doped $LiBH_4$ sample after rehydrogenation at 400 °C under 10 MPa H_2 for 12 h was performed, as seen in Fig. 6(b). It could be found that over 7.0 wt% hydrogen could be released in the second dehydrogenation for the 30 mol% h-BN doped $LiBH_4$ sample. And the the rehydrogenation capacity of the composites is about 6 wt% during the third dehydrogenation. In other words, experimental results of this work showed that the rehydrogenation properties of $LiBH_4$ were improved by h-BN addition in terms of rehydrogenation conditions and rehydrogenation percentage than that of ball milled $LiBH_4$.

In the SEM examinations of ball milled $LiBH_4$ and 30 mol% h-BN doped $LiBH_4$ samples, appreciable difference on the $LiBH_4$ particle morphology was observed between ball milled $LiBH_4$

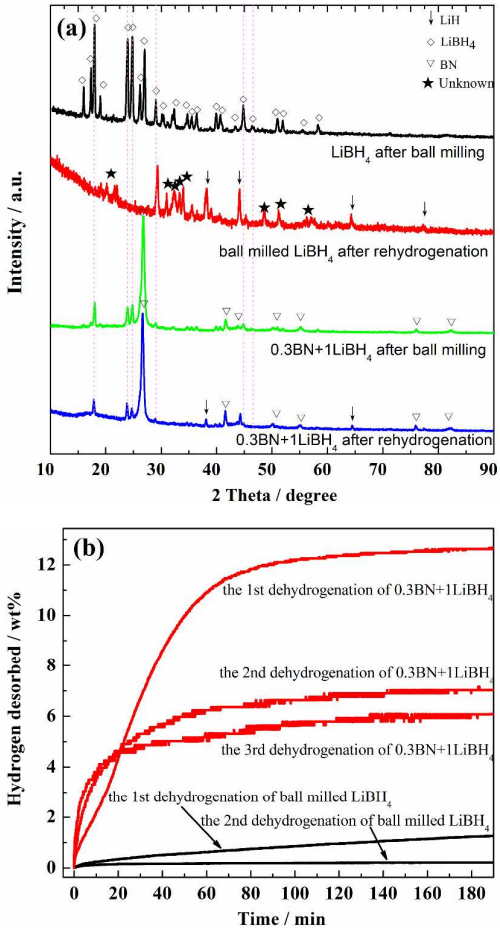

Fig. 6 XRD patterns and isothermal dehydrogenation curves of ball milled $LiBH_4$ and 30 mol% h-BN doped $LiBH_4$ samples after rehydrogenation under 400 °C and 10 MPa of H_2 for 12 h.

and $LiBH_4$ doped with h-BN. As shown in Fig. 7(a), ball milled $LiBH_4$ particles are not small. Even after ball milling for 3h, the particles size is over 2 μm, because of the agglomerations reunited after ball milling. Interestingly, after ball milling with 30 mol% h-BN, $LiBH_4$ particles become much smaller than 2 μm, dispersing on h-BN flat surface, as shown in Fig. 7(c). It is believed that decreasing particle size is beneficial to enhance dehydrogenation of $LiBH_4$[31, 32]. Fig. 7(b) and (f) show the SEM images of ball milled $LiBH_4$ and 30 mol% doped $LiBH_4$ after dehydrogenation at 400 °C. Obviously, after dehydrogenation, the ball milled $LiBH_4$ decomposition product (B and LiH) particles agglomerated together to form larger clusters. For 30 mol% h-BN doped $LiBH_4$ sample, the decomposition product particles size does not increase. In this regard, the h-BN additives might play a role as effect heterogeneous nucleation site for the decomposition and prevent the nucleated particles from further growth during dehydrogenation reaction[33]. These might be largely credible explanation for why the dehydrogenation and rehydrogenation properties of $LiBH_4$ are improved by doping with h-BN.

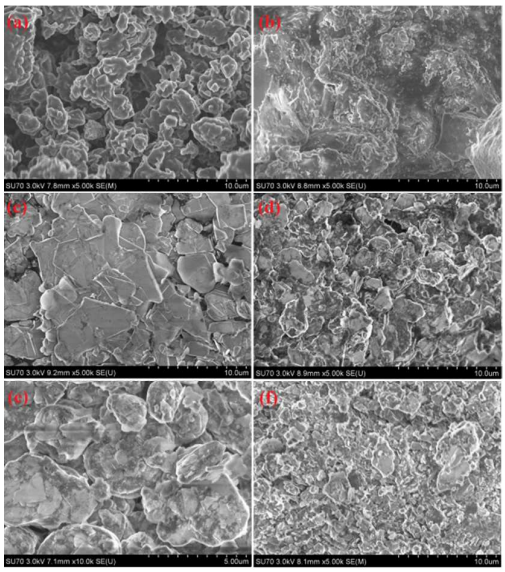

Fig. 7 SEM images of a) ball milled $LiBH_4$ sample, b) ball milled $LiBH_4$ sample after dehydrogenation at 400 °C, c) neat h-BN, d) 30 mol% h-BN doped $LiBH_4$ sample after ball milling and f) 30 mol% h-BN doped $LiBH_4$ sample after dehydrogenation at 400 °C.

Based on the above analyses, the whole process of synthesis and de/rehydrogenation for $LiBH_4$ doped with h-BN systems from a micro point of view is illustrated in Scheme 1. After $LiBH_4$ ball milled with h-BN sheets, $LiBH_4$ particles become small and well disperse on the surface of h-BN. The lone pair electrons of N atom on the surface of h-BN induces part of $LiBH_4$ destabilization, resulting in the onset of dehydrogenation of $LiBH_4$ was decreased to 180 °C with a small amount of hydrogen desorption, which also could be supported by the dehydrogenation of $LiBH_4$ doped with graphite as shown in the ESI Fig.S2† During the dehydrogenation process, the $LiBH_4$ covered on the surface of h-BN will decomposes firstly, and then the products of $LiBH_4$ decomposition (LiH and B particles) play the role of the nucleation sites. And with effect heterogeneous nucleation site of h-BN, the product particles of $LiBH_4$ decomposition are more inclined to dispersing on the surface of h-BN. In the rehydrogenation process, the composites can reverse to form $LiBH_4$ in short distance on the surface of h-BN.

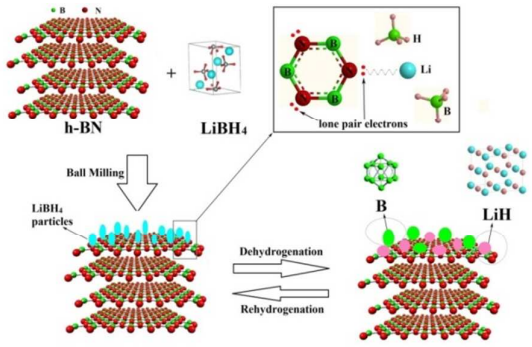

Scheme 1 Illustration of the process of synthesis and de/rehydrogenation for $LiBH_4$ doped with h-BN systems

4. Conclusions

The effects of h-BN additives on the dehydrogenation and rehydrogenation properties of $LiBH_4$ were investigated. The results show that the dehydrogenation kinetics of $LiBH_4$ is greatly improved by doping with h-BN. For instance, 30 mol% h-BN doped $LiBH_4$ can release 12.6 wt% hydrogen in 2h at 400 °C, while only 0.98 wt% H_2 is gained for ball milled $LiBH_4$. The onset dehydrogenation temperature of $LiBH_4$ is reduced to 180 °C from 280 °C of ball milled $LiBH_4$, the apparent activation energy of hydrogen desorption has been reduced from 198.31 kJ/mol for ball milled $LiBH_4$ to 155.8 kJ/mol for $LiBH_4$ doped with 30 mol% h-BN. Meanwhile, over 7.0 wt% hydrogen can be rehydrogenated at 400 °C under 10 MPa H_2. XRD, SEM and TEM analyses demonstrate that h-BN remain stable in the ball milling process and de/rehydrogenation. It is believed that h-BN dopant services as effect heterogeneous nucleation site for dehydrogenation of $LiBH_4$ and plays a role in preventing the nucleated particles from further growth. Besides, the presupposition complex reaction between the lone pair electrons of N atom on surface of h-BN with "electron-deficient" molecule $LiBH_4$ induces destabilization of $LiBH_4$ might take effect on improving the dehydrogenation of $LiBH_4$.

Acknowledgments

The authors gratefully acknowledge the financial supports for this research from the National High Technology Research & Development Program of China (2012AA051503), the National Natural Science Foundation of China (51471151, 51171173), the Program for Innovative Research Team in University of Ministry of Education of China (IRT13037), and the Zhejiang Provincial Science & Technology Program of China (2014C31134)

References:

1 A. Zuttel, S. Rentsch, P. Fischer, P. Wenger, P. Sudan, P. Mauron and C. Emmenegger, *Journal of Alloys and Compounds*, 2003, **356**, 515-520.
2 L. Schlapbach and A. Zuttel, *Nature*, 2001, **414**, 353-358.
3 A. Züttel, A. Borgschulte and S. I. Orimo, *Scripta Materialia*, 2007, **56**, 823-828.
4 Y. Yan, A. Remhof, S.-J. Hwang, H.-W. Li, P. Mauron, S.-i. Orimo and A. Zuttel, *Physical Chemistry Chemical Physics*, 2012, **14**, 6514-6519.
5 F. Pendolino, P. Mauron, A. Borgschulte and A. Züttel, *Journal of Physical Chemistry C*, 2009, **113**, 17231-17234.
6 P. Ngene, P. Adelhelm, A. M. Beale, K. P. de Jong and P. E. de Jongh, *Journal of Physical Chemistry C*, 2010, **114**, 6163-6168.
7 A. Züttel, P. Wenger, S. Rentsch, P. Sudan, P. Mauron and C. Emmenegger, *Journal of Power Sources*, 2003, **118**, 1-7.
8 J. F. Mao, Z. Wu, X. B. Yu, T. Don, T. J. Chen, B. C. Weng, J. Ni, N. X. Xu and T. S. Huang, *Rare Metal Materials and Engineering*, 2007, **36**, 2248-2250.
9 M. Meggouh, D. M. Grant and G. S. Walker, *Journal of Physical Chemistry C*, 2011, **115**, 22054-22061.
10 J. Xu, Y. Li, J. Y. Cao, R. R. Meng, W. C. Wang and Z. D. Chen, *Catalysis Science & Technology*, 2015, **5**, 1821-1828.

11 J. Yang, A. Sudik and C. Wolverton, *Journal of Physical Chemistry C*, 2007, **111**, 19134-19140.
12 G. L. Xia, X. B. Yu and Z. Wu, *Rare Metal Materials and Engineering*, 2009, **38**, 1618-1621.
13 B. J. Zhang and B. H. Liu, *International Journal of Hydrogen Energy*, 2010, **35**, 7288-7294.
14 B. J. Zhang, B. H. Liu and Z. P. Li, *Journal of Alloys and Compounds*, 2011, **509**, 751-757.
15 Y. H. Guo, X. B. Yu, L. Gao, G. L. Xia, Z. P. Guo and H. K. Liu, *Energy & Environmental Science*, 2010, **3**, 465-470.
16 T. Sun, H. Wang, Q. G. Zhang, D. L. Sun, X. D. Yao and M. Zhu, *Journal of Materials Chemistry*, 2011, **21**, 9179-9184.
17 Z. G. Zhang, H. Wang and M. Zhu, *International Journal of Hydrogen Energy*, 2011, **36**, 8203-8208.
18 H.-W. Li, Y. Yan, S.-i. Orimo, A. Züttel and C. M. Jensen, *Energies*, 2011, **4**, 185-214.
19 H. Liu, L. Jiao, Y. Zhao, K. Cao, Y. Liu, Y. Wang and H. Yuan, *Journal of Materials Chemistry A*, 2014, **2**, 9244-9250.
20 X. B. Yu, D. M. Grant and G. S. Walker, *Journal of Physical Chemistry C*, 2009, **113**, 17945-17949.
21 X. B. Yu, D. A. Grant and G. S. Walker, *Journal of Physical Chemistry C*, 2008, **112**, 11059-11062.
22 M. Q. Fan, L. X. Sun, Y. Zhang, F. Xu, J. Zhang and H. L. Chu, *International Journal of Hydrogen Energy*, 2008, **33**, 74-80.
23 J. Greim and K. A. Schwetz, in *Ullmann's Encyclopedia of Industrial Chemistry*, Wiley-VCH Verlag GmbH & Co. KGaA, 2000, DOI: 10.1002/14356007.a04_295.pub2.
24 I. Smith and R. P. Lerner, *Folia Primatologica*, 1971, **14**, 110-117.
25 J. P. Soulie, G. Renaudin, R. Cerny and K. Yvon, *Journal of Alloys and Compounds*, 2002, **346**, 200-205.
26 H. E. Kissinger, *Analytical Chemistry*, 1957, **29**, 1702-1706.
27 P. A. Ward, J. A. Teprovich, B. Peters, J. Wheeler, R. N. Compton and R. Zidan, *Journal of Physical Chemistry C*, 2013, **117**, 22569-22575.
28 J. Shao, X. Z. Xiao, X. L. Fan, L. T. Zhang, S. Q. Li, H. W. Ge, Q. D. Wang and L. X. Chen, *Journal of Physical Chemistry C*, 2014, **118**, 11252-11260.
29 S. Orimo, Y. Nakamori, G. Kitahara, K. Miwa, N. Ohba, S. Towata and A. Züttel, *Journal of Alloys and Compounds*, 2005, **404–406**, 427-430.
30 P. Mauron, F. Buchter, O. Friedrichs, A. Remhof, M. Bielmann, C. N. Zwicky and A. Züttel, *Journal of Physical Chemistry B*, 2008, **112**, 906-910.
31 M. Christian and K. F. Aguey-Zinsou, *Nanoscale*, 2010, **2**, 2587-2590.
32 X. F. Wan and L. L. Shaw, *Acta Materialia*, 2011, **59**, 4606-4615.
33 Z. Z. Fang, X. D. Kang and P. Wang, *International Journal of Hydrogen Energy*, 2010, **35**, 8247-8252.